Journal of Applied Polymer Science

Evaluation of New Chemically Modified Coconut Shell Adsorbents with Tannic Acid for Cu (II) Removal from Wastewater

Vicente de Oliveira Sousa Neto,[1] Diego Quadros Melo,[2] Talles Cardoso de Oliveira,[2] Raimundo Nonato, P. Teixeira,[3,4] Marcos Antônio Araújo Silva,[5] Ronaldo Ferreira do Nascimento[2,4]

[1]Universidade Estadual do Ceará, Centro de Ciências e Tecnologia da Região do Inhamuns, CECITEC. BR 116, s/n, Bairro Bezerra e Souza, Tauá-Ceará Brazil, CEP 63600000

[2]Departamento de Química Analítica e Físico Química Campus do Pici, Universidade Federal do Ceará, Centro de Ciências, Bloco 940-CEP 60451-970, Fortaleza, Ceará

[3]Departamento de Química Biológica—Rua Cel. Antônio Luis, Universidade Regional do Cariri, 1161—63.100-000—Pimenta, Crato, Ceará, Brazil

[4]Departamento de Engenharia Hidráulica e Ambiental, Universidade Federal do Ceará, Campus do Pici-Centro de Tecnologia, Bloco 713—CEP 60451-970, Fortaleza, Ceará, Brazil

[5]Departamento de Física, Universidade Federal do Ceará, Campus do Pici—Bloco 922, CEP 60.455-900, Fortaleza, Ceará, Brazil

Correspondence to: R. F. Nascimento (E-mail: ronaldo@ufc.br)

ABSTRACT: The adsorption of Cu (II) from aqueous solutions using coconut shell modified powder was investigated in batch experiments. The surface charge of the adsorbent was determined. The points of zero charge (PZC) of the adsorbents (pH_{PZC}) were 4.5, 2.0, and 2.0 to raw coconut (RC), raw coconut alkalized (RCA), and coconut shell modified with tannic acid (TCA) adsorbent, respectively. Batch experiments were performed under kinetic and equilibrium conditions. The kinetic data were analyzed using a pseudo second-order, and Elovich equation. Adsorption equilibrium data were investigated using the Langmiur, Freundlich, Temkin, and Dubinin–Raduschevich (D–R) isotherm models. It has been found that chemically modified coconut shell (TAC) affected performance when compared with unmodified coconut shell (RC). Kinetic studies showed that the adsorption followed a pseudo-second-order rate model. Biosorption kinetics of Cu(II) on the adsorbent TCA was rapid such that almost 90% of Cu(II) were adsorbed within 80 min. © 2014 Wiley Periodicals, Inc. J. Appl. Polym. Sci. **2014**, *131*, 40744.

KEYWORDS: adsorption; cellulose and other wood products; fibers; kinetics; theory and modeling

Received 25 November 2013; accepted 20 March 2014

DOI: 10.1002/app.40744

INTRODUCTION

The ground and surface waters pollution by chemical contaminants is a worldwide problem. Toxic metal contamination of water sources is hazardous to plants, animals and microorganism, and can be carcinogenic to mankind.[1,2] On the other hand, metals are playing important roles in most industries. Copper for instance is used in engine moving parts, brake linings, metal plating, fungicides, insecticides, etc.[3,4] It is a biological poison. Acute exposure to large doses could be harmful for human and required control of exposure.[5] Presence of higher concentrations (>5 mg L^{-1}) in the body has been linkage many of health problems such as kidney damage, high fever, hemolysis, and vomiting.[6] Excessive copper in the marine system has been found to damage marine life and damage the gills, liver, kidneys, the nervous system, and changing sexual life of fishes.[7]

Research interest into the production of cheaper adsorbents to replace costly wastewater treatment methods such as chemical precipitation, ion-exchange, electroflotation, membrane separation, reverse osmosis, electrodialysis, solvent extraction, etc. are attracting attention of scientists.[8] Adsorption is one the physicochemical treatment processes found to be effective in removing toxic metal ions from aqueous solutions, and the main advantages of the biosorption process, when compared with currently used methods, include low operational costs, minimization of the volume of chemical to be disposed. Several mechanisms may govern biosorption of metal ions that differ qualitatively and quantitatively from species to species, origin, and processing procedure of biomass/biomaterials.

An adsorbent can be considered as cheap or low-cost if it is abundant in nature, requires little processing and is a byproduct of waste material from waste industry.[9] In Brazil, the coconut

shell is a lignocellulosic biomass, which is an agricultural waste generates of large production, and its disposal is an environmental problem. Biomass/biomaterials comprise several chemical or functional groups such as acetamido, amino, amide, sulfhydryl, sulfate, and carboxyl, hydroxyl, etc. which could attract and sequester the metal ions from solution. However, the utilization of coconut shell as biosorbent has been considered a technology alternative and economically viable for the treatment of wastewater containing metal ions.[10–12]

In this context, most of the adsorption studies for metal ions removal have been focused in the use of raw biomasses or treated with acid-base solutions for increase their adsorption capacity, thus biomasses such as papaya wood,[13] coconut bagasse,[10,14] maize leaf,[15] alginate,[16] lalang leaf powder,[17] sugar cane bagasse,[18,19] moringa,[20] and passion fruit skin,[21] have been investigated.

Thus, this study was aimed to investigate the feasibility of using coconut shells modified with tannic acid (TCA) as an efficient bioadsorbent for copper ion removal from water and industrial wastewater. The advantage of the modification with tannic acid is the introduction of hydroxyl groups for increase the adsorption capacity, and it has a relatively low cost and easily can be obtained on the market, because it is very used by industries to pharmaceutical and food. The sorption is often described by adsorption isotherm and modeling of isotherms is the best way to predict and compare sorption performance by adsorbent. Four isotherm models were used to predict adsorbent performance using synthetic and industrial wastewater solutions of Cu (II). The dynamic behavior of Cu (II) sorption onto the TAC was also investigated from experimental data with kinetic models and diffusion models using wastewater.

EXPERIMENTAL

Adsorbent

Raw coconut shell (RC) was obtained from EMBRAPA (Fortaleza-Ce- BRAZIL). The coconut shells was ground and screened to prepare 59 to 100 mesh size particles. The fractions were further dried in an oven with air circulation at 60°C for a period of 24 h. Reagent such as copper sulphate, tannic acid, sodium hydroxide of analytical grade (Merck, São Paulo), and buffer acetate at pH 5.5 were used.

Alkaline Treatment of Raw Coconut Shell (RCA)

The coconut shell powder was treated with NaOH (0.1*M*) and heated at 70°C for 1 h under 150 rpm stirring. The solid material was filtered, washed several times with distilled water and dried at 60°C for 48 h.

Preparation of Coconut Shells Modified with Tannic Acid (TCA)

Into glass flask containing raw coconut shell alkalized (RCA) an adequate amount of tannic acid 0.5 mol L^{-1}, and distilled water were added, and the resulting mixture aqueous solution was heated to 70°C. The reaction was stopped after the required time by cooling the resulting mixture to room temperature (28 ± 2°C). The material was filtered and exhaustedly washed with water to remove the unreacted tannic acid and by products. The dried sample of TCA was sieved and the fraction with average particle diameter of 60 to 100 mesh was collected and used for all the adsorption experiments.

FT-IR and Zero Potential Charge Analysis

The FT-IR spectra of the coconut shell (unmodified and modified) were obtained using the pressed disc technique infrared spectroscopy using a FTLA 2000-102, ABB-BOMEM equipment from ABB Inc. (Quebec, QC/Canada). The samples were prepared by mixing 10 mg of material with 990 mg of spectroscopy grade KBr (Merck, São Paulo). A Zetasizer Nano ZS instrument (Malvern, GBR) was used to measure the zeta potentials of all of the samples.

Cu (II) Solutions and Waste Water Batch

A series of batch experiments were conducted to study the mechanism, isotherm, and kinetics of adsorption. A stock solution (500 mg L^{-1}) of Cu (II) was prepared by dissolving $CuSO_4.5H_2O$ (analytical reagent) in deionized water. The acetate buffer(pH 5.5) was prepared with sodium acetate and glacial acetic acid. The tests were performed in duplicate. The Cu (II) concentrations were measured using an Atomic Absorption Spectrophotometer GBC 933 plus model from Varian, Inc. Corporate (Palo Alto, CA).

Adsorption Isotherm. Coconut shells modified with tannic acid (TCA) (50.0 mg) were added to solutions (25.0 mL) in 100 mL erlenmeyer flasks, with Cu (II) concentrations in the range of 40 to 320 mg L^{-1}. The mixtures were mechanically stirred (150 rpm) for 2 h at room temperature (28 ± 2°C). The data obtained of the adsorption isotherm for monoelement systems were described according to Langmuir, Freundlich, Temkin and Dubinin–Raduschevich (D–R) models.

The equilibrium adsorption capacities were calculated by the differences between initial and final concentrations at any given time to according by eq. (1):

$$qe = \frac{(C_o - C_e)}{W} V \quad (1)$$

where q_e is the equilibrium adsorption capacity (mg g^{-1}), C_o is the initial concentration of the metal ion in mg L^{-1}, C_e is the equilibrium concentration of metal ion in mg L^{-1}, V is the volume of the solution in liters, and W is the mass of adsorbent in grams.

Adsorption Kinetic. A Cu (II) solution (100.0 mg L^{-1}) was continuously shaken (150 rpm) at pH 5.5. Aliquots of the supernatant were collected in regular periods of time, up to 120 min. The adsorption capacity of the adsorbent at any given time was calculated with eq. (1).

Industrial Effluent. An industrial effluent from plating rinsing process of the electroplating industry (Juazeiro do Norte, CE, Brazil) with an original chemical composition containing Cu^{2+} (30,000 mg L^{-1}), SO_4^{2-} (46,500 mg·L^{-1}), and Cl^- (234 mg $L^{-1)}$ was used as a stock solution to adsorption study. The electroplating wastewater was diluted to 500 mg L^{-1} Cu^{2+} at pH 1.2 and it was employed as stock solution in the adsorption isotherm studies. The kinetic and isotherm experiment was also performed using industrial effluent the same conditions the synthetic effluent.

Table I. Surface Characteristics of Raw Coconut

Raw coconut (RC)	
N_2 adsorption	
Superficial area specific-BET(m^2 g^{-1})	218
Average pore diameter BJH (Å)	34.0

RESULTS AND DISCUSSION

Physical and Chemical Characterization of the Adsorbent

The physical characterization of the coconut shells is shown in Table I. Specific surface area was 218.0 m^2 g^{-1} and pore size distribution (BJH) was 34 Å, indicating a characteristic of mesoporous materials.

Modification of the Adsorbent Before/After Alkali Treatment

Sodium hydroxide is a well-known fiber-swelling agent. Alkaline treatment on cellulose is irreversible process and leads to a change in supramolecular structure and its morphology, facilitating their solubilization. The alkaline treatment also removes components such as lignin and hemicelluloses and confers greater solubility cellulose due keep out the formation of intramolecular bonds.[22,23] It can be observed in Figure 1 that the alkaline pretreated modified adsorbent promotes a little performance to RC, and good performance to TCA adsorbent when compared with modified adsorbent not submitted to alkaline pretreatment.

Two different packing structures of cellulose chain (type I and type II) can be formed.[24] It is possible that the conversion of cellulose type I to type II has a considerable efficient in the presence of NaOH solution. Cellulose is transformed to sodium cellulose by treatment with concentrated NaOH solution, and then reverts to cellulose by washing. During this process, smaller hydrates of the sodium hydroxide dipole penetrate into the cellulose crystalline regions and destroy the strong intermolecular. Thus, the increase in adsorption capacity on coconut shell submitted to alkaline treatment can be attributed to the formation of cellulose type II, which has more hydroxyl group available to react with the metal.[24]

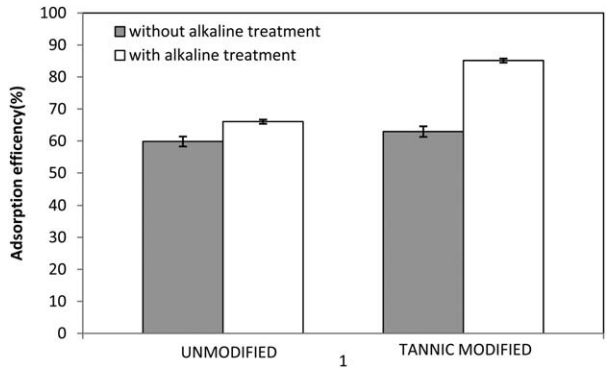

Figure 1. Alkali treatment effect on adsorption efficiency. Experimental conditions: [Cu (II)] = 100 mg L^{-1} , size adsorbents: 60 to 100 mesh, speed agitation: 150 rpm, pH = 5.5 buffer acetate.

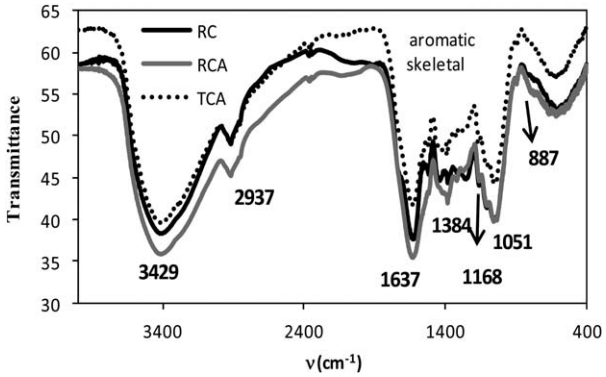

Figure 2. The FT-IR spectra of raw coconut shell (RC) raw coconut treated with alkaline solution (RCA) treatment, and coconut shells modified with tannic acid (TCA).

FT-IR Analysis

The FT-IR spectrum of raw coconut shells (RC) displays a number of absorption peaks (Figure 2), which indicates the presence of different types of functional groups in the biosorbent. In Figure 2 the peaks at 3429, 2937, 1637, 1384, 1051, and 887 cm^{-1} are associated with cellulose. A strong band at 3429 cm^{-1} is attributed to the stretching of hydroxyl groups (alcohol/phenol) which is consistent with the peaks at 1072 and 1168 cm^{-1} assigned to alcoholic C–O. The absorption at 2937 cm^{-1} arises from C–H stretching. The small absorbance at 1607, 1511, 1427, and 1323 cm^{-1} (shown in the circle) correspond to the aromatic skeletal vibrations, ring breathing with C–O stretching in lignin. The peak at 1637 cm^{-1} can be attributed to adsorbed water and oxygen-containing group. The bands at 1384 and 1247 cm^{-1} (no shown) are attributed to absorption by C–H and C–O stretching in acetyl group in hemicelluloses, respectively. The strong band at 1051 cm^{-1} is assigned to C–O stretching in cellulose, hemicelluloses, and lignin or C–O–C stretching in cellulose and hemicelluloses. The small sharp band at 887 cm^{-1} is originated from the β-glucosidic linkages between the sugar units in hemicelluloses and cellulose.

In the Figure 3 is shown the FT-IR spectrum of coconut shells modified with tannic acid (TCA) doped with Cu (II). The peak located at 1737 cm^{-1} is characteristic of carbonyl group stretching from carboxylic acid or ester groups. In general, the absorption by carbonyl bonds in esters gives a peak at 1750 cm^{-1}, and

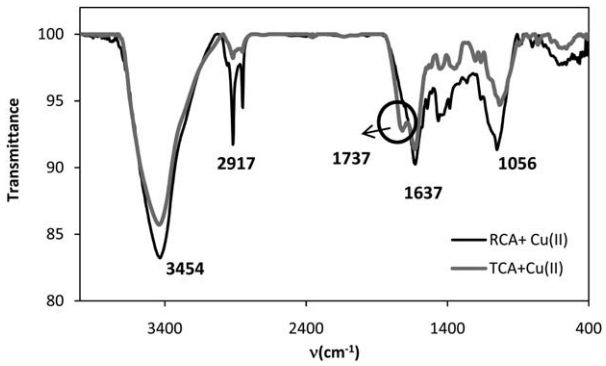

Figure 3. The FT-IR spectra of RCA and TCA after copper adsorption.

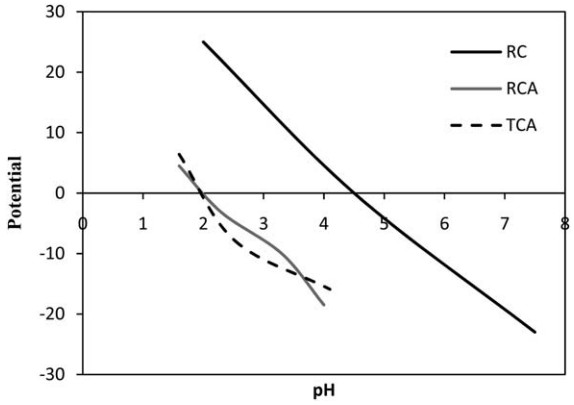

Figure 4. Zeta potential of the adsorbents. Experimental conditions: [Cu (II)] = 100 mg L^{-1} , contact time: 2 h, size adsorbents: 60 to 100 mesh, speed agitation: 150 rpm, pH= 5.5 buffer acetate.

one in carboxylic acids exhibits a band at 1712 cm^{-1}. The two bands are strongly overlapped and therefore resulted in a peak centered at 1737 cm^{-1}.The peak at 1257 cm^{-1} can be attributed to the C–O stretching of phenolic groups.[14] The FT-IR spectrum for copper loaded biosorbent showed that the intensity of some peaks were shifted or substantially lower than those before biosorption, suggesting the participation of –OH, –COO−, and $–NH_2$ in the binding of copper by coconut. Sousa Neto et al.,[14] suggest that the mechanism of copper binding on coconut shell could also occur by surface complexation.

Effect of pH on the Adsorption

The points of zero charge (PZC), Figure 4, of the adsorbents (pH_{PZC}) were 4.5, 2.0, and 2.0 to RC, RCA, and TCA adsorbent, respectively. After modification is noted that pH_{PZC} was shift from 4.5 (RC) to 2.0 (RCA and TC). Below pH_{PZC}, the surface is positively charged under these conditions the uptake of metal ions would be quite low due to electrostatic repulsion. With increasing pH (beyond PZC) the negative charge on the surface of adsorbent increases thereby enhancing the metal ion adsorption.

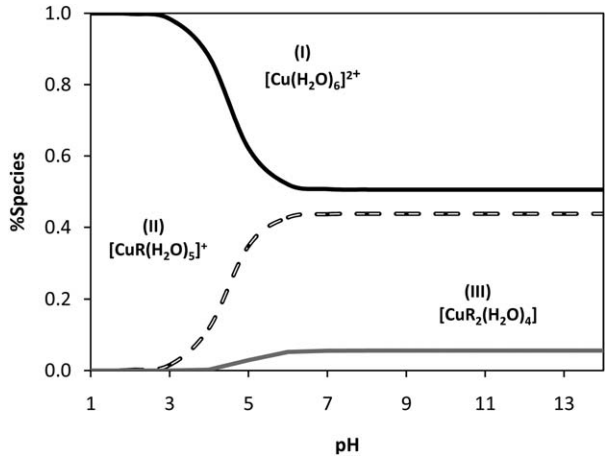

Figure 5. Distribution of species in solution as a function of pH where R = acetate group CH_3COO^-. Acetic acid concentration (5.0×10^{-3} mol L^{-1}). The complex constants were obtained from reference (Harris, 2005). [25]

Table II. Comparison of Adsorption Characteristics of RCA and TCA at Different Initial Concentrations (pH 5.5, Contact Time of 180 min, [Cu (II)] = 40–320 mg L^{-1}, temperature: 28 ± 2°C)

	RCA		TCA	
C_o (mg L^{-1})	q_e (mg g^{-1})	%	q_e (mg g^{-1})	%
40	14.99	79.95	18.46	92.30
80	26.77	23.23	36.66	91.65
120	30.10	21.96	50.8	84.66
180	34.21	29.78	61.8	79.77
200	38.57	20,27	76.00	55.62
240	38.88	18.19	83.05	52.54
280	43.44	19.23	90.3	35.93
320	46.37	29.29	94.5	34.06

The adsorption depends on the nature of the surface of the adsorbent and the type of the metal species in the water solution. The type of the species of Cu (II) in the water solution depends strongly on the pH. The copper species on solution can be found in Figure 5. It can be shown by stability constant that in the presence of CH_3COO^-, at pH range 5.0 to 5.5, charge species I and II are dominant.[25] In this work to keep out $[H^+]$ competition and it was choose pH 5.5.

Effect of Initial Concentration

The initial concentration effect was investigated and the results are shown in Table II. As seen from Table II, the adsorption capacity and RCA and TCA (synthetic effluent) increases with increasing initial concentration of Cu (II). However, it shows a decrease of the yield. The increase in the adsorption capacity of the adsorbents with increased initial concentration of Cu (II) can be due to the higher driving force. When the initial Cu (II) concentration was increased from 40 to 320 mg L^{-1}, the adsorption capacity in equilibrium, q_e, increased from 14.99 to 46.27 mg g^{-1} for RCA and 18.46 to 94.5 mg L^{-1} for TCA. The adsorption capacity doubled after modification.

Adsorption Isotherm

An adsorption isotherm is characterized by certain constant values, which express the surface properties and affinity for the adsorbent and can also be used to compare the adsorption capacities of the adsorbent for different pollutants.

The mechanisms related to the adsorption of Cu (II), for synthetic batch onto RC and TCA, and industrial batch onto TCA, were investigated using Langmuir, Freundlich, Temkin, and Dubinin–Redushkevich (D–R) isotherm models. For this were tested the experimental data with the parameters obtained using linear regression. In order to compare the validity of isotherm model more definitely, a normalized deviation, $\Delta q_e\%$, is calculated as follows:

$$\Delta q_e = \frac{\sum_{i=1}^{N} \left| \frac{q_{e,i,\exp} - q_{e,i,cal}}{q_{e,i,\exp}} \right|}{N} \times 100 \quad (2)$$

where $q_{e,\exp}$ and $q_{e,cal}$ are the amount of metal ion adsorbed experimental and calculated at equilibrium and N, the number of measurements.

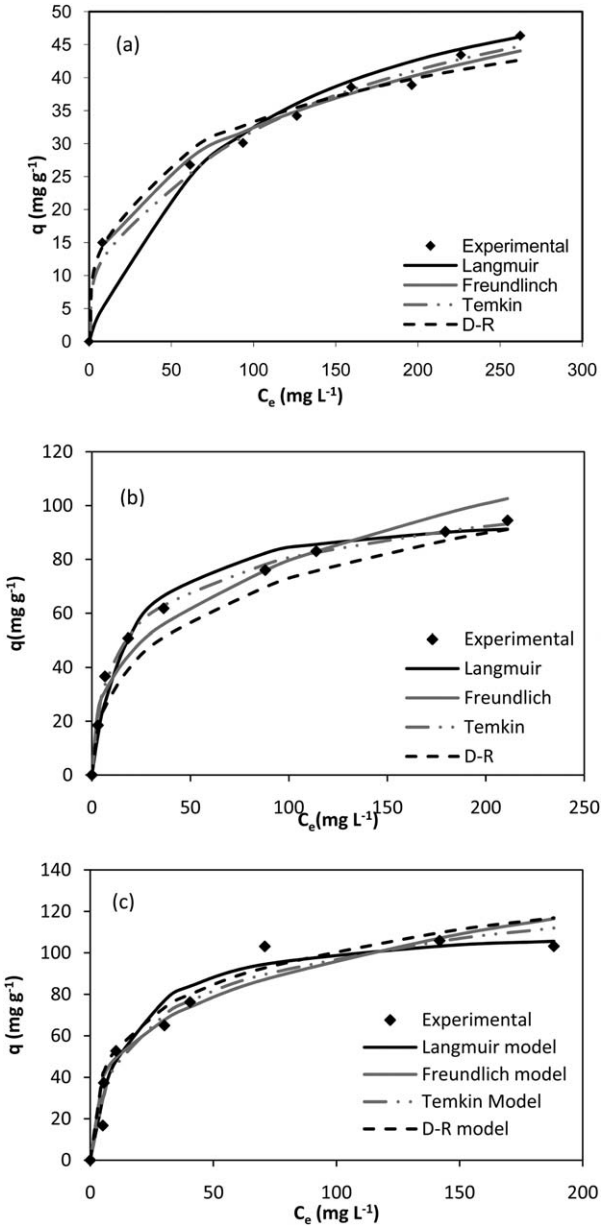

Figure 6. Theoretical isotherms and experimental data for adsorption of Cu (II) synthetic batch onto (a) RCA, (b) TCA, and (c) industrial batch onto TCA at pH 5.5, contact time of 180 min.

The adsorption isotherms obtained are shown in Figure 6, and the parameters calculated for the models used are presented in Table III.

Langmuir Isotherm. The Langmuir model is based on the assumption that maximum adsorption corresponds to a saturated monolayer of solute molecules on the adsorbent surface, with no lateral interaction between the adsorbed metal.[26] The expression of the Langmuir model is given by eq. (3):

$$q_e = \frac{q_{\max} k_L C_e}{(1 + k_L C_e)} \tag{3}$$

where q_e (mg g^{-1}) and C_e (mg L^{-1}) are the amount of metal ion adsorbed per unit mass of sorbent and metal concentration in solution at equilibrium, respectively. $q_{\max}$ is the maximum amount of the metal per unit mass of sorbent to form a complete monolayer on the surface bound at high k_L is a constant related to the affinity of the binding sites (L mg^{-1}). The Langmuir equation can be described by linearized form as shown in eq. (4).

$$\frac{C_e}{q_e} = \frac{1}{q_{\max}} C_e + \frac{1}{q_{\max} k_L} \tag{4}$$

The values of maximum adsorption capacity were obtained from the slope of the plot of C_e/q_e versus C_e. Efficient adsorbents are expected to have high k_L and $q_{\max}$ values. The values of k_L and $q_{\max}$ followed the order: TCA (industrial) > TCA (synthetic) > RCA (synthetic). The highest values of k_L and $q_{\max}$ for TCA indicate a higher performance for the Cu (II) sorption.

Coconut shell modified investigated in this study exhibited for copper sorption capacity higher compared to results found in literature for others biosorbents.[10,19,27–29]

The essential feature of Langmuir model can be expressed in terms of a dimensionless constant separation factor (R_L) given by the following eq. (5):

$$R_L = \frac{1}{1 + k_L C_0} \tag{5}$$

where k_L is the Langmuir constant (L mg^{-1}) and C_0 is the initial Cu (II) concentration (mg L^{-1}). It has been established that for favorable adsorption, $0 < R_L < 1$; unfavorable adsorption, $R_L > 1$; linear adsorption, $R_L = 1$; and adsorption process is irreversible if $R_L = 0$.

The values of R_L lie between 0.04 and 0.31 for the initial Cu (II) concentration range from 40 to 320 mg L^{-1} indicating favorable adsorption of Cu (II) onto TAC. It is possible write the Langmuir isotherm in dimensionless form as eq. (6).

$$y = \frac{x}{R_L + (1 - R_L)x} \tag{6}$$

where

$$y = \frac{q_e}{q_{\max}} \text{ and } x = \frac{C_e}{C_0}$$

In eq. (4) if $R_L < 1$, then the solute strongly prefer the solid phase over the fluid phase indicating good efficiency of adsorption. If R_L is greater than 1, the isotherm has a concave shape that the solute prefers the fluid phase over solid phase.[31] The case for $R_L = 1$ corresponds to a linear isotherm ($y = x$). The Figures 7 and 8 show the dimensionless Langmuir isotherm for RCA and TCA adsorbent at 28 ± 2°C, respectively. Figure 8 shows that TCA adsorbent has better adsorption performance than RCA adsorbent. It is occurs because in the initial Cu (II) concentration the RCA ($R_L = 0.862$) shows a curve similar to linear isotherm case ($R_L = 1$) indicating a poor performance in low Cu (II) concentration. On the other hand the TCA adsorbent ($R_L = 0.309$) shows a two convex shape indicating a good performance in adsorbent process for the initial, and final copper concentration ($R_L = 0.043$).

Freundlich Isotherm. The Freundlich isotherm is an empirical equation employed to describe heterogeneous systems.[32] The Freundlich equation is expressed as eq. (7):

Table III. Langmuir, Freundlich, Temkin, and Dubinin–Redushkevich (D–R) Isotherm Model Constants and Correlation Coefficients for Adsorption of Cu (II) Synthetic Batch onto RC and TCA, and Industrial Batch onto TCA for 28 ± 2°C

		Synthetic batch		Industrial batch
Models	Parameter	RCA	TCA	TCA
Langmuir	q_e (mg g^{-1})	62.5	99.0	113.6
	k_L (mg L^{-1})	1.08×10^{-2}	5.60×10^{-2}	7.0×10^{-2}
	R^2	0.978	0.995	0.993
	Δq_e%	8.34	2.64	9.66
Freundlich	n	3.14	2.90	3.40
	k_F ($mg^{1-(1/n)}$ $L^{1/n}$ g^{-1})	7.48	16.0	25.0
	R^2	0.988	0.939	0.939
	Δq_e%	0.39	3.62	17.34
Temkin	ΔH (kJ mol^{-1})	−8.61	−13.5	−13.85
	k_T (L mg^{-1})	0.109	1.04	1.15
	R^2	0.963	0.996	0.932
	Δq_e%	2.17	1.13	9.35
D-R	q (mg g^{-1})	82.1	206	221
	E (kJ mol^{-1})	12	15.8	18.3
	κ (mol^2 J^{-2})	3.46×10^{-9}	4.00×10^{-9}	3.00×10^{-9}
	R^2	0.970	0.964	0.955
	Δq_e%	0.55	0.71	18.57

$$q_e = K_F C_e^{1/n} \quad (7)$$

where q_e is the equilibrium amount adsorbed (mg g^{-1}), C_e the equilibrium concentration of the adsorbate (mg L^{-1}). K_F and n are Freundlich constants related to adsorption capacity and intensity of adsorption, respectively. Freundlich equation can be described by linearized form as shown in eq. (8):

$$\ln(q_e) = \ln(k_F) + \frac{1}{n}\ln(C_e) \quad (8)$$

The values of k_F and $1/n$ were calculated from the intercept and slope of the plot between $\ln q_e$ versus $\ln C_e$. The parameters (k_F, $1/n$) and the correlation coefficient (R^2) obtained by the Freundlich isotherm are given in Table III. It is well-known that favorable adsorption processes are associated to "n" values between 2 and 10.[3] "n" was found to be in this range for adsorbents studied. RCA and TCA have a high k_F and n compared to results found in literature for other biosorbents in similar operational condition (e.g., pH and temperature).[33–36]

Temkin Isotherm. The Temkin isotherm equation assumes that the heat of adsorption of all the solutes in the layer decreases linearly with coverage due to adsorbent–adsorbate interactions,[37] and that the adsorption is characterized by a uniform distribution of the binding energies, up to some maximum binding energy. Temkin model is given by, eq. (9):[38]

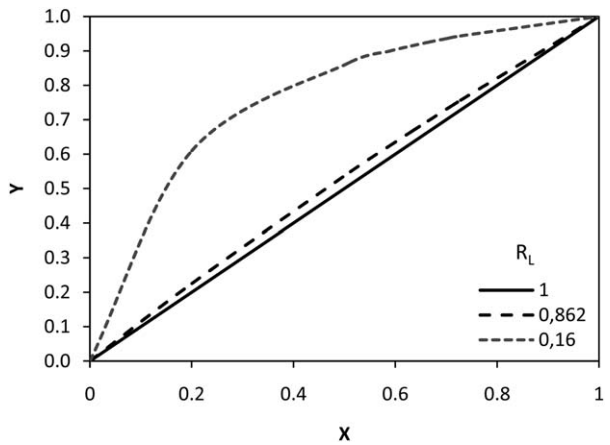

Figure 7. The dimensionless Langmuir isotherm: adsorption of Cu (II) onto RCA adsorbent at 28°C.

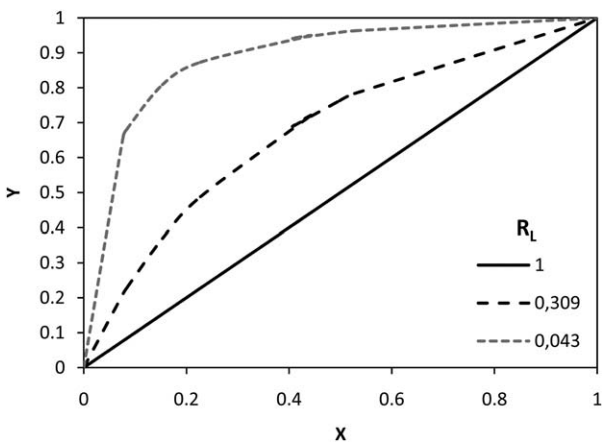

Figure 8. The dimensionless Langmuir isotherm: adsorption of Cu (II) onto TCA adsorbent at 28°C.

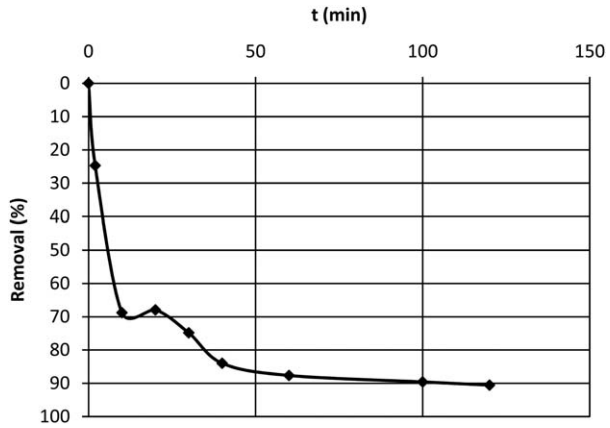

Figure 9. Effect of contact time on the Cu (II) sorption by TCA. Condition: [Cu (II)] = 100 mg L^{-1} , acetate buffer pH = 5.5.

$$\theta = \frac{RT}{\Delta Q}\ln(k_T) + \frac{RT}{\Delta Q}\ln(C_e) \quad (9)$$

where θ is the fractional coverage ($\frac{q_e}{q_m}$), q_e is the amount of ions metals adsorbed at equilibrium (mg g^{-1}), q_m is the monolayer capacity of the adsorbent (mg g^{-1}), R the universal gas constant (kJ mol^{-1} K^{-1}), T the temperature (K), $\Delta Q = (-\Delta H)$ the variation of adsorption energy (kJ mol^{-1}), and k_T is the Temkin equilibrium constant (L mg^{-1}).

If the adsorption process obeys Temkin equation, the variation of adsorption energy and the Temkin equilibrium parameters (Table III) can be calculated from the slope and the intercept of the plot θ versus ln (C_e) [eq. (9)]. The ΔH value found to RCA and to TCA indicates exothermic process. In the industrial batch the ΔH (kJ mol^{-1}) value was negative to TCA which suggests the occurrence of heat release. This behavior was similar to synthetic batch conditions.

Dubinin–Redushkevich (D–R) Isotherm. The equilibrium data were also applied to the D–R model to determine the type of sorption (physical or chemical).[39] The non-linear form of D–R isotherm is presented as the following eq. (10):

$$q_e = q_m \exp(-k\varepsilon^2) \quad (10)$$

which it can be linearized as, eq. (11):

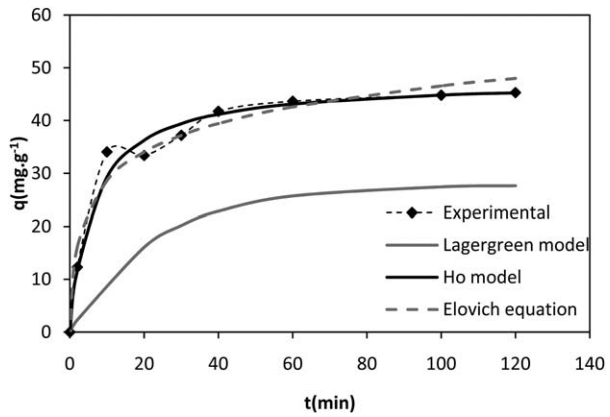

Figure 10. Kinetics of Cu (II) adsorption on TCA. Conditions: [Cu (II)] = 100 mg L^{-1} in Industrial batch; pH = 5.5 acetate buffer.

$$\ln(q_e) = \ln(q_m) - k\varepsilon^2 \quad (11)$$

where q_e is the amount of Cu (II) adsorbed onto per unit dosage of adsorbent (mol g^{-1}), q_m is the theoretical monolayer sorption capacity (mol g^{-1}), and k is the constant of the sorption energy (mol^2 J^{-2}), which is related to the average energy of sorption per mole of the adsorbate as it is transferred to the surface of the solid from an infinite distance in the solution. The parameter ε is the Polanyi potential which can be obtained by eq. (12), where T is the solution temperature (K) and R is the gas constant, which is equal to 8.314 (J mol^{-1} K^{-1}).[40]

$$\varepsilon = RT\ln\left(1 + \frac{1}{C_e}\right) \quad (12)$$

The sorption energy, E (kJ mol^{-1}), can be calculated from eq. (13) using the D–R parameter k:

$$E = \frac{1}{\sqrt{-2k}} \quad (13)$$

The mean energy of sorption, kJ mol^{-1}, is the free energy involved in the transfer of 1 mol of solute from solution to the surface of the adsorbent. D–R parameters to RCA and TCA adsorbents are shown in Table III. The value of mean sorption energy gives information about chemical and physical sorption. The E value ranges from 1 kJ mol^{-1} to 8 kJ mol^{-1} for physical sorption and from 8 kJ mol^{-1} to 16 kJ mol^{-1} for chemical sorption.[41] The E values found to RCA and to TCA (synthetic and industrial wastewater) indicate that the type of sorption of Cu (II) is chemical sorption to both adsorbents. It was 15.80% higher than synthetic batch conditions. Figure 6(b,c) show theoretical isotherms and experimental data for adsorption of Cu (II) synthetic batch, and industrial batch onto TCA.

According to Table III, the values found for deviations were low. The experimental data for the RCA adsorbent were best fitted the Freundlich model, while for TCA follows the Langmuir model. This suggests the same energy of binding sites for TCA. Models of Temkin and D–R also showed low deviations suggesting that above mentioned data by these models can also be used.

Adsorption Kinetics

The kinetic studies help in predicting the progress of adsorption, but the determination of the adsorption mechanism is also important for design purposes. In a solid–liquid adsorption process, the transfer of the adsorbate is controlled by either boundary layer diffusion (external mass transfer) or intra-particle diffusion (mass transfer through the pores), or by both. In the kinetic study was applied kinetic models and diffusion models to adsorption Cu (II) onto TCA adsorbent using industrial batch.

The initial phase of biosorption was rapid (Figure 9). In approximately 10 min about 70% of Cu (II) are removed from the solution. However, 10 min after removal does not change. Forty minutes from the start of the adsorbent removed about 84% of all Cu (II), reaching phase equilibrium in 80 min with 90% removed. The adsorbent proved to be efficient, with an initial high rate of Cu (II) removal in a short time interval.

Pseudo-First-Order Kinetic Model. Lagergren,[42] suggested a rate equation for the sorption of solutes from a liquid solution. This pseudo first-order rate equation is:

Table IV. Kinetic Models Parameters for Adsorption of Cu (II) Industrial Batch onto TCA for 28 ± 2°C

		TCA adsorbent
Experimental Ho model	q_e	45.3
	q_{cal} (mg g^{-1})	47.6
	k_2 (g mg^{-1} min^{-1})	3.35×10^{-3}
	R^2	0.999
Elovich equation	q_{cal} (mg g^{-1})	47.9
	α (mg g^{-1} min^{-1})	30.5
	β (g mg^{-1})	0.128
	R^2	0.970
Lagergren model	q_{cal} (mg g^{-1})	27.64
	k_1 (min^{-1})	4.31×10^{-2}
	R^2	0.972

Conditions: Cu (II) concentration 100 mg L^{-1}, pH = 5.5, acetate buffer.

$$\ln(q_e - q_t) = -k_1 t + \ln(q_e) \quad (14)$$

where q_e (mg g^{-1}) is the adsorption capacity at the equilibrium, q_t (mg g^{-1}) is the individual capacity in a given time, k_1 (min^{-1}) is the pseudo-first order rate constant and t is the time in minutes.

The value of the sorption rate constant (k_1) for Cu (II) adsorption by TCA can be determined from the plot of ln ($q_e - q_t$) against t. The experimental q_e value did not agree with the calculated one (q_{cal}), Figure 10. The results (Table IV) indicated that pseudo first order model was unable to describe the time-dependent Cu (II) sorption by TCA.

Pseudo-Second-Order Kinetic Model. Several kinetic models have described reaction orders in sorption systems. A pseudo-second-order kinetic model has been considered to be the most appropriate.[43] The rate equation for the reaction may be represented by the following expression:

$$\frac{dqt}{dt} = k_2(q_e - q_t)^2 \quad (15)$$

where k_2 is the sorption rate constant (g mg^{-1} min^{-1}), q_e (mg g^{-1}) is the amount of metal ions sorbed in the equilibrium, and q_t is the amount of metal ions on the sorbent surface at any time t. The sorption rate can be calculated as the initial sorption rate when t approaches zero. The pseudo-second-order equation can be written as:

$$\frac{t}{qt} = \frac{1}{k_2 q_e^2} + \frac{1}{q_e} t \quad (16)$$

The linear plot of (t/q_t) versus t gave ($1/q_e$) as the slope and ($1/k_2 q_e^2$) as the intercept. This procedure is more likely to predict the behavior over the whole range of adsorption. The linear plot of t/q_t versus t (no shown) indicated a good agreement between the experimental (q_e) and the calculated (q_{cal}) values (Figure 10). Values of kinetic parameters are listed in Table IV for the adsorption of Cu (II) ions onto TCA.

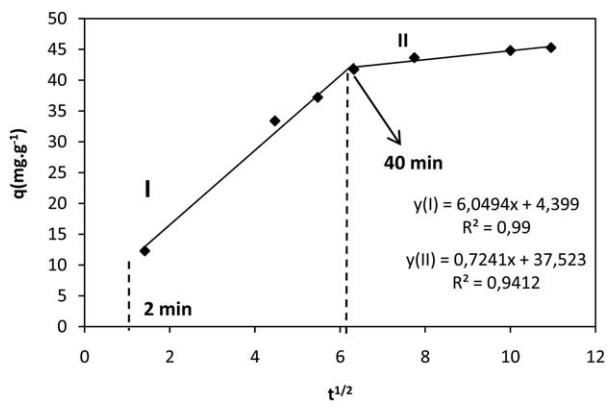

Figure 11. Intraparticle diffusion plots for the Cu (II) (Industrial bath) adsorption on TCA for initial concentration 100 mg L^{-1} at pH 5.5 (acetate buffer).

Elovich Equation. Elovich equation[44] is generally expressed as:

$$\frac{dqt}{dt} = \alpha e^{-\beta qt} \quad (17)$$

where, α initial adsorption rate (mg g^{-1} min^{-1}); β, desorption constant (g mg^{-1}) during any one experiment. To simplify Elovich equation, Chien and Clayton,[45] assumed $\alpha\beta t >> t$ and by applying boundary conditions ($q_t = 0$ at $t = 0$ and $q_t = q_t$ at $t = t$), eq. (18) becomes nonlinear form:

$$q_1 = \frac{1}{\beta}\ln(1 + \alpha\beta t) \quad (18)$$

After linearization eq. (18) can be expressed as follows [eq. (19)].

$$q_t = \frac{1}{\beta}\ln(\alpha\beta) + \frac{1}{\beta}\ln(t) \quad (19)$$

where α and β are obtained from the slope and intercept of the linear plot of q_t versus ln(t). The q_e values calculated from Elovich equation agreed quite well with the experimental values (Figure 10). Elovich parameters are shown in Table IV.

Mechanism Study

An intraparticle diffusion process tends to control the adsorption rate in systems characterized by high concentrations of adsorbate, good mixing, and big particle size of adsorbent.[46] In order to gain insight into the mechanisms and rate-controlling steps affecting the kinetics of adsorption, the kinetic experimental results were fitted to the Webber's intra-particle diffusion model and Boyd's diffusion model.[47–49]

Weber-Morris's Model. Weber's intraparticle diffusion model[47] can be expressed as,

$$q_t = k_{id} t^{1/2} + C \quad (20)$$

where C is the intercept and k_{id} is the intraparticle diffusion rate constant (mg/g $min^{1/2}$), which can be evaluated from the slope of the linear plot of q_t versus $t^{1/2}$. The values of provide information about the thickness of the boundary layer. In general, the larger the intercept, the greater is the boundary layer effect.[50]

If intraparticle diffusion is controlling, then q_t versus $t^{1/2}$ will be linear, and if the plot passes through the origin, then the rate

Table V. Results for the Sorption of Cu (II) onto TCA

Webber-Morris' pore-diffusion model					
		I		II	
K_I (mg g^{-1} min^{-1})	C_1 (mg g^{-1})	D (cm^2 min^{-1})	K_I (mg g^{-1} min^{-1})	C_2 (mg g^{-1})	D (cm^2 min^{-1})
6.05	4.40	1.95×10^{-6}	0.720	37.5	2.80×10^{-8}
Boyd's diffusion model					
	I		II		
B	$D_{(I)}$ (cm^{-2} min^{-1})	R^2	B	$D_{(I)}$ (cm^{-2} min^{-1})	
0.095	3.02×10^{-6}	0.968	0.038	1.21×10^{-6}	

Obtained by the Weber-Morris Diffusion Model and Boyd's Diffusion Model using the linear method

limiting process is due only to intraparticle diffusion. Otherwise, some other mechanism along with intra-particle diffusion must also be involved. Pore-diffusion plots often show several linear segments. It has been proposed that these linear segments represent pore-diffusion in pores of progressively smaller sizes.[51] Eventually, equilibrium is reached, and adsorption (q_e) stops changing with time, and a final horizontal line is established at q_e. When points in a group are identified as belonging to a linear segment, linear regression can then be applied to these points, and the corresponding k_{id} is estimated.

In eq. (20), k_{id} (mg g^{-1} min$^{-1/2}$) is defined as the intra-particle diffusion rate constant and is related to the intraparticle diffusivity D_i (cm min^{-1}), in the following way.

$$k_{id} = \left(\frac{3q_e}{dp}\right)\sqrt{\frac{D_i}{\pi}} \tag{21}$$

where d_p (cm) is the particle diameter and q_e (mg g^{-1}) is the solid phase concentration at equilibrium. As seen in Figure 11, the points were not linear over the whole time range, implying that more than one process affected the adsorption, and this deviation might be due to the difference in the mass transfer rate for the initial and final stage of adsorption. This indicates that diffusion into one class of pores was not the only rate-limiting mechanism in the adsorption process. Applying Weber-Morris' model in the step (I) and II the values of k_{id}(I), $D_{i(I)}$, $C(I)$, and R^2 were obtained , Table V. The breakpoint in Figure 11 is at 40 min.

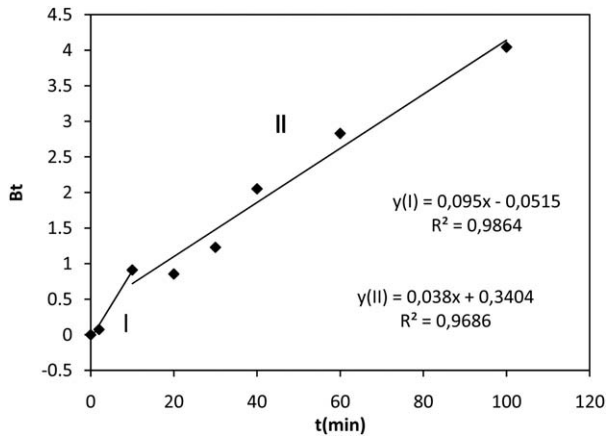

Figure 12. Boyd plot for adsorption of Cu (II) (Industrial batch) onto TCA and initial feed concentration 100 mg L^{-1} at pH 5.5 (acetate buffer). In step I, $F < 0.85$, eq. (24) was applied; in step II, $F > 0.85$, eq. (25) was applied.

Boyd Model. To determine whether the adsorption process occurs via external diffusion or an intraparticle mechanism, the kinetic data were investigated by the Boyd model.[48,49] If diffusion inside the pores is the rate limiting step, then the results can be expressed as eq. (22):

$$F = 1 - \left[\frac{6}{\pi^2}\right]\sum_{n=1}^{\infty}\left(\frac{1}{n^2}\right)\exp\left(-\pi^2 Bt\right) \tag{22}$$

where B is a constant, and F is the fractional attainment of equilibrium at different times t given by eq. (23):

$$F = \frac{q_t}{q_e} \tag{23}$$

and q_t and q_e are the Cu(II) uptakes (mg g^{-1}) in equilibrium, at a time t. The term B_t is calculated by the following equations of Reichenberg.[52]

$$F > 0,85 \quad B_t = -0,4977 - \ln(1-F) \tag{24}$$

$$F < 0,85 \quad B_t = \left(\sqrt{\pi} - \sqrt{\left(\pi - \frac{\pi^2 F}{3}\right)}\right)^2 \tag{25}$$

In order to apply this model, the product term B_t is calculated for each value of F, and then the resulting B_t values are plotted against t (Boyd plot), as given in Figure 12. If the plot is linear,

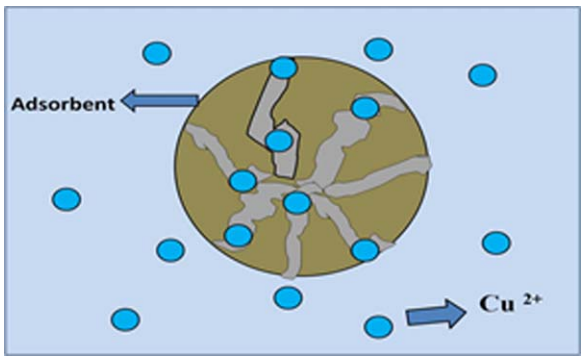

Scheme 1. Schematic adsorption process. [Color figure can be viewed in the online issue, which is available at wileyonlinelibrary.com.]

Table VI. Langmuir Parameters for Bioadsortion of Cu (II) by Various Kinds of Biosorbents

Sorbent	Operational conditions		q_{max} (mg g^{-1})	Reference
	pH	T (°C)		
Lignin	5.5	20	22.9	27
Sour orange residue (SOR)	4.5	28	52.1	28
Coconut	6.0		40.98	56
Moringa oleifera leaves powder	5.0	20-40	167.9	58
Orange peel	5.5	30	70.73	57
Sugarcane bagasse	5.0	-	184.9	55
	5.0	28	31.53	19
Barley straw	7.0	-	31.71	59
Mimosa tannin gel	5.0	25	43.7	30
Nonliving green algae *Cladophora fascicularis*	5,0	25	102	29
Coconut shell (TCA)	5.5	28	99.0	This study

then the slope is equal to B, and it can be concluded that pore-diffusion is the rate-controlling step. The effective diffusion coefficient, D_i, (cm^2 s^{-1}) can be calculated from eq. (26) where d (cm) is particle diameter.

$$B = \left(\frac{\pi^2 D_i}{d^2}\right) \tag{26}$$

Linear segments can also be obtained by Boyd plots, and in such case every segment is analyzed separately to obtain the corresponding diffusion coefficient.

In this study the Morris-Webber model does not allowed take any conclusion as to the time interval between 0 and 2 min. It was not possible know with precision any step in this time interval which can pass through the origin indicating a stage of intra pore diffusion in the initial stages of adsorption. In the graph of B_t versus t (step I), Figure 12, on a line passes near the origin suggesting a stage intra pore diffusion. In a second step the linear coefficient was slightly different from zero which suggests an intraparticle diffusion. Table V shows the typical results for the sorption of copper ions onto TCA obtained by Webber–Morris's model, and Boyd model using the linear method.

Cu (II) adsorption results obtained by others researchers for the modified biomass were compared in agreed Langmuir adsorption capacity as seen in Table VI. According to results the coconut shells modified (TCA) investigated in this study have a adsorption capacity for Cu (II) greater than other material such as sugar cane modified,[19,53–55] coconut,[11,56] and orange peel.[57] By other hand the bioadsorbents such as moringa oleifera[58] and green algae[29] have a capacity greater than the modified materials tested in this study for Cu (II) at pH 5 (Table VI).

CONCLUSIONS

Tannic acid was used to modify the surface of coconut shell. The Cu (II) removal from synthetic aqueous solution, and industrial aqueous solution by modified coconut shells was found to be effective. Cu (II) removal was greater for treated coconut shell with tannic acid than for coconut submitted alkaline treatment. Equilibrium adsorption data showed good fits to the isotherms of Langmuir, Freundlich, Temkin, and Dubinin–Raduschevich. Adsorption process followed a second-order kinetic model, and intra-particle diffusion was not only rate controlling step. The results show that the coconut shell modified with tannic acid can be applied for the removal of Cu (II) from wastewater.

ACKNOWLEDGMENTS

The authors are grateful to Dra. Regina Celia Monteiro de Paula by the PZC measurements and Department of Physical and Analytical Chemistry from Federal University of Ceara (UFC) for providing laboratory facilities. This work was supported by CAPES, FUNCAP, and CNPQ (Process No.: 576591/2008-4 and 306114/2008-9).

REFERENCES

1. Boddu, V. M.; Abburi, K.; Randolph, A. J.; Smith, E. D. *Separate Sci. Technol.* **2008**, *43*, 1365.
2. Barros, F. C. F.; Sousa, F. W.; Cavalcante, R. M.; Carvalho, T. V.; Dias, F. S.; Queiroz, D. C; Vasconcellos, L. C. G.; Nascimento, R. F. *Clean* **2008**, *36*, 292.
3. Melo, D. Q.; Neto, V. O. S.; Oliveira, J. T.; Barros, A. L.; Gomes, E. C. C.; Raulino, G. S. C.; Longuinotti, E.; Nascimento, R. F. *J. Chem. Eng. Data* **2013**, *58*, 798.
4. Jaishankar, M.; Mathew, B. B.; Shah, M. S.; Krishna, M. T. P.; Sangeetha, G. K. R. *J. Environ. Pollut. Hum Health* **2014**, *2*, 1.
5. Hossain, M. A.; Ngo, H. H.; Guo, W. S.; Nguyen, T. V. *Bioresour. Technol.* **2012**, *113*, 97.
6. Bhattacharyya, K. G.; Gupta, S. S. *Separate Sci Technol.* **2006**, *50*, 388.
7. Teixeira, R.; Sousa Neto, V. O.; Oliveira, J. T.; Melo, D. Q.; Silva, M. A.; Nascimento, R. F. *Bioresources* **2013**, *8*, 3356.
8. Sousa, F. W.; Sousa Neto, V. O.; Teixeira, R. N. P.; Fechine, P. B. A.; Freire, P. T. C.; Silva-Araujo, M. A.; Nascimento, R. F. In Electroplating; Darwin Sebayang, D., Hasan, S. B. H., Eds.; InTech, Rijeka, **2012**, Chapter 5, p 107.
9. Parmar, M.; Thakur, L. S. *Int. J. Plant Anim. Enviromen. Sci.* **2013**, *3*, 143.
10. Pino, G. H.; Mesquita, L. M. S.; Torem, M. L.; Pinto, G. A. S. *Miner. Eng.* **2006**, *19*, 380.
11. Sousa, F. W.; liveira, A. G.; Ribeiro, J. P.; Keukeleire, D.; Sousa, A. F.; Nascimento, R. F. *Desalin. Water Treat.* **2011**, *36*, 289.
12. Sousa Neto, V. O.; Teixeira, R. N. P.; Silva, M. A.; Freire, P. T. C.; Keukeleire, D.; Nascimento, R. F. *Bioresources* **2011**, *6*, 3376.
13. Saeed, A.; Akhter, M.W.; Iqbal, M. *Separate Sci Technol.* **2005**, *45*, 25.
14. Sousa Neto, V. O.; Carvalho, T. V.; Honorato, S. B.; Gomes, C. L.; Barros, F. C. F.; Araújo-Silva, M. A.; Freire, P. T. C.; Nascimento, R. F. *Bioresources* **2012**, *7*, 1504.

15. Babarinde, N. A. A.; Babalola, J. O.; Sanni, R. A. *Int. J. Phys. Sci.* **2006**, *1*, 23.
16. Lim, S. -F.; Zheng, Y. -M.; Zou, S. -W.; Chen, J. P. *Environ. Sci. Technol.* **2008**, *42*, 2551.
17. Hanafiah, M. A. K.; Ngah, W. S. W.; Zakaria, H.; Ibrahim, S. C. *J. Biol. Sci.* **2007**, *7*, 222.
18. Sousa, F. W.; Silva, M. J. B.; Oliveira, I. R. N.; Oliveira, A. G.; Cavalcante, R. M.; Fechine, P. B. A.; Sousa Neto, V. O.; Keukeleire, D.; Nascimento, R. F. *J. Environ Manage.* **2009**, *1*, 1.
19. Dos Santos, V. C. G. J.; De Souza, V. T. M.; Tarley, C. R. T.; Caetano, J.; Dragunski, D. C. *Water Air Soil Pollut.* **2011**, *216*, 351.
20. Meneghel, A. P.; Gonçalves, A. C., Jr.; Rubio, F.; Dragunski, D. C.; Lindino, C. A.; Strey, L. *Water Air Soil Pollut.* **2013**, *224*, 1383.
21. Gerola, G. P.; Vilas Boas, N.; Caetano J.; Tarley, T. C. R.; Gonçalves, A. C., Jr.; Dragunski, D. C. *Water Air Soil Pollut.* **2013**, *224*, 1446.
22. Zhang, L.; Ruan, D.; Gao, S. *J. Polym. Sci. Part B: Polym. Phys.* **2002**, *40*, 521.
23. Jin, H.; Zha, C.; Gu, L. *Carbohydr. Res.* **2007**, *342*, 851.
24. Kroon-Batenburg, L. M. J.; Kroon, J. *Glycoconjug. J.* **1997**, *14*, 677.
25. Harris, D. C. Quantitative Chemical Analysis 6th ed.; LTC: Rio de Janeiro, **2005**; p 809.
26. Langmuir, I. *J. Am. Chem. Soc.* **1916**, *38*, 2221.
27. Guo, X.; Zhang, S.; Shan, X. *J. Hazard. Mater.* **2008**, *151*, 134.
28. Khormaei, M.; Nasernejad, B.; Edrisi, M.; Eslamzadeh, T. *J. Hazard. Mater.***2007**, *149*, 269.
29. Deng, L.; Su, Y.; Su, H.; Wang, V.; Zhu, X. *Adsorption.* **2006**, *12*, 267.
30. Şengil, I.A.; Özacar, M.; Türkmenler, H. *J. Hazard. Mater.* **2009**. *162*, 1046.
31. Cooney, D. O. Adsorption Design for wastewater treatment CRC Press: Boca Raton, FL, **1999**; p 208.
32. Freundlich, H. Z. *Phys. Chem.* **1907**, *57*, 385.
33. Vijayaraghavan, K.; Palanivelu, K.; Velan, M. *Bioresour. Technol.* **2006**, *97*, 1411.
34. Cay, S.; Uyanik, A.; Ozasik, A. *Separ Sci Technol.* **2004**, *38*, 273.
35. Djeribi, R.; Hamdaoui, O. *Desalination.* **2008**, *225*, 95.
36. Amarasinghe, B. M. W.; Williams, R. A. *Chem. Eng. J.* **2007**, *132*, 299.
37. Temkin, M.; Pyzhev, V. *Acta Phys. Chim.* **1940**, *12*, 217.
38. Hamdaoui O.; Naffrechoux E. *J. Hazard. Mater.* **2007**, *147*, 381.
39. Dubinin, M.M. *Chem. Rev.* **1960**, *60*, 235.
40. Polanyi, M. *Verh. Dtsch. Phys. Ges.* **1914**, *16*, 1012.
41. Sarı, A.; Tuzen, M.; Cıtak, D.; Soylak, M. *J. Hazard. Mater.* **2007**, *148*, 387.
42. Lagergren, S. K. *Svenska Vetenskapsakad. Handl.* **1898**, *24*, 1.
43. Ho, Y. S.; McKay, G. *Process Biochem.* **1999**, *34*, 451.
44. Roginsky, S. Z.; Zeldovich, J. *Acta Phys. Chim.* **1934**, *1*, 554.
45. Chienand, S. H.; Clayton, W. R. *Soil Sci. Soc. Am. J.* **1980**, *44*, 265.
46. Mohan, D.; Singh, K.P. *Water Res.* **2002**, *36*, 2304.
47. Weber, W.J., Jr.; Morris, J.C. *J. Sanit Eng. Div.* **1963**, *31*, 31.
48. Boyd, G. E.; Adamson, A. W.; Myers, L.S. Jr. *J. Am. Chem. Soc.* **1947**, *69*, 69, 2836.
49. Boyd, G. E., Schubert, J.; Adamson, A. W. *J. Am. Chem. Soc.* **1947**, *69*, 2818.
50. Kavitha, D.; Namasivayam, C. *Bioresour. Technol.* **2007**, *98*, 14.
51. Hameed, B. H.; Tan, I. A. W.; Ahmad, A. L. *Chem. Eng. J.* **2008**, *144*, 235.
52. Reichenberg, D. *J. Am. Chem. Soc.* **1953**, *75*, 589.
53. Karnitz, O. Jr.; Gurgel, L. V. A.; Melo, J. C. P.; Botaro, V. R.; Melo, T. M. S.; Gil, R. P. F.; Gil, L. F. *Bioresour. Technol.* **2007**, *98*, 1291.
54. Said, A.; Aly, A.; El-Wahab, M.; Soliman, S.; El-Hafez, A.; Helmey, V.; Goda, M. *J. Water Resour. Protein* **2013**, *5*, 10.
55. Homagai, P. L.; Ghimire, K. N.; Inoue, K. *Bioresour. Technol.* **2010**,*101*, 2067.
56. Vieira, A. P.; Santana, S. A. A.; Bezerra, C. W. B.; Silva, H. A. S.; Chaves, J. A. P.; Melo, J. C. P.; Silva Filho, E. C.; Airoldi, C. *J. Hazard. Mater.* **2009**,*166*,1272.
57. Feng, N., Guo, X. T. *Nonferr. Metal Soc.* **2012**, *22*, 1224.
58. Reddy, D.H.K.; Seshaiaha, K.; Reddy, A. V. R.; Lee, S. M. *Carbohydr. Polym.* **2012**. *88*, 1077.
59. Pehlivan, E.; Altun, T.; Parlayici, Ş. *Food Chem.* **2012**, *135*, 2229.